JOURNAL OF Applied Polymer SCIENCE

Crystallization and Fracture Behaviors of High-Density Polyethylene/Linear Low-Density Polyethylene Blends: the Influence of Short-Chain Branching

Guanghao Shen, Hongwang Shen, Banghu Xie, Wei Yang, Mingbo Yang
College of Polymer Science and Engineering, Sichuan University, 610065, China
Correspondence to: B. Xie (E-mail: xiebanghu@scu.edu.cn)

ABSTRACT: Two commercial polyethylene samples, linear high-density polyethylene (HDPE) and branched linear low-density polyethylene with almost the same molecular weight distribution but different contents of short-chain branching (SCB) were melt blended based on the consideration of practical application. Dynamic rheology analysis indicated good compatibility of all the blends with different compositions. Common differential scanning calorimeter (DSC) tests and successive self-nucleation and annealing (SSA) treatment showed several interesting phenomena. First, without consideration of the effect of molecular weight and molecular weight distribution impact, co-crystallization occurred at all ratios even the two components had a considerable difference in SCB distribution. Second, in SSA curves the area of the first two melting peaks, i.e., the amount of the thick lamellas of the two components showed an obvious positive deviation with the increase of HDPE content owing to the crystal perfection improved by the co-crystallization. Essential Work of Fracture tests proved the co-crystallization effects had a positive effect on the improvement of the resistance to crack propagation. © 2013 Wiley Periodicals, Inc. J. Appl. Polym. Sci. 129: 2103–2111, 2013

KEYWORDS: blends; polyolefins; crystallization

Received 23 September 2012; accepted 18 September 2012; published online 7 January 2013
DOI: 10.1002/app.38937

INTRODUCTION

Polyethylene (PE) is one of the most conventional and versatile resins widely used in tube, packaging, film and so on.[1] Normally, molecular structure parameters including molecular weight, molecular weight distribution, branch content, branch length, and branch distribution will determine the crystallization behavior and service property of PE. These factors are all dependent on the type of monomer, catalysis, comonomer ratio, and polymerization mechanism used during the polymerization.[2–4]

To overcome the difficulty to adjust some important properties, many studies had been carried out on the PE blends with bimodal molecular weight distribution (BPE), which has received wide attention and industry usage.[5–10] The high molecular weight fraction with higher degree of branching endows BPE products with better toughness and environmental stress crack resistance, while the low molecular weight fraction with more linear chain structure assures the good processability of the resin.

The polydispersity of polymer is reflected in not only molecular weight distribution but also the distribution of branch points (or the density of branching). Thus, no doubt it's worth finding out that will the polymer blends with a "bimodal chain branch distribution" characteristic also show any novel performance?

Naturally, these materials can all be seen as polymer blends of two or more parent polymers with different chain structures. Therefore, the crystallization behavior and mechanical property of the blends might be influenced by both the properties of the two parent polymers. Multiple factors including chain structures of two components, blending methods etc. make it really difficult to study the influence of one single factor on the blend. Many studies have been carried out on the miscibility and crystallization behavior of these blends.[11–31] Choi et al.[11,12] claimed that a certain extent of phase separation would happen if the content of short-chain branching (SCB) reached a critical value after investigating a series of PE blend samples. Tashiro et al.[13–15] tracked the crystallization of the blend of deuterated high-density polyethylene (HDPE) and branch PE with different SCB contents and found that the two kinds of PE were miscible not only at molten state but also in the crystalline phase with the formation of co-crystallization. Cho et al.[16] found that even LDPE/linear low-density polyethylene (LLDPE) blend was incompatible at crystalline phase, HDPE/LLDPE blend were

miscible at both molten and crystalline states. With DSC, SAXS, WAXS ways, Rana[17] studied the crystallization behavior of linear PE blend with different branched PE samples and found that the two components nucleated respectively but grew together. Zhao et al.[18] also studied HDPE/LLDPE blends with similar methods and found that the occurrence of co-crystallization. The degree of co-crystallization was determined by the SCB content of the branched PE and affected by composition of the blend. Their results were consistent with later researches by Tanem et al.[19,20]

In recent years, thermal fractionation methods such as step crystallization, successive self-nucleation, and annealing (SSA), temperature rising elution fractionation and crystallization analysis fractionation have found wide use in predicating the aggregation state of PE blends.[21–27] For SSA, especially, with shorter time and better resolution,[25,28–31] it can be used to reveal the relationship between crystallization behaviors and branched structures of the blend. It solves the problem in common DSC test that the melting and crystallization peak of one component might overlap with the other.

It is worth noting that facing the matter that the aggregated state structure is affected by various elements, many articles have to choose materials with very narrow molecular weight distribution but low molecular weight (around 100,000 g/mol or even much lower).[11–15] Nevertheless, commercial PE materials are much different from those materials. In this condition, it is hard to eliminate the influences of molecular weight distribution and to focus on the effect of SCB. Meantime, among those trying to figure out the relationship between chain structures and aggregated structures of PE blends, few people focused on the final mechanical properties and the relationship with chain structures.

In practical application, after a long service time, traditional PE usually breaks at a stress far below the yield limit for the poor ability to resist environmental stress cracking and crack propagation. In this aspect, it is very important to predict or to characterize the ability of PE materials on the resistance of environmental stress cracking and crack propagation. The Essential Work of Fracture (EWF) method has found its wide application in characterizing fracture toughness of polymers.[32–35]

In this article, we aim to further uncover the relationship between SCB and phase structures of PE blends and their impact on the fracture behavior. We chose a HDPE sample and a LLDPE sample with almost the same molecular weight distribution but considerable difference in the SCB content. By blending these two materials together, the blends show "bimodal chain branch distribution" and a normal unimodal molecular weight distribution. By SSA and other methods, the crystallization behavior at different blend ratios was studied and related with the fracture property to further understand the underlying mechanism.

EXPERIMENTAL

Materials

HDPE 5000S (ρ = 0.951 g/cm^3) and LLDPE 7042N (ethylene/1-butylene copolymer, ρ = 0.920 g/cm^3) were purchased from Lanzhou Petrochemical Co. China. SCB content is 16 CH_3/1000C for LLDPE, and 3 CH_3/1000C for HDPE.

Sample Preparation

A TSSJ-25 co-rotating twin screw extruder (L/D=33) was used in blending HDPE and LLDPE at mass ratios of 0 : 100, 10 : 90, 30 : 70, 50 : 50, 70 : 30, and 100 : 0; named H0, H10,H30, H50, H70, H100, respectively. Temperature profiles were 165, 200, 205, and 200°C from the feed zone to the die. All the samples were extruded twice so as to ensure the mixing uniformity. To avoid the melt from oxidative degradation, 0.5% of antioxygen 1010 was added.

After extrusion, all the samples were dried and melt-pressed into 25 mm × 1 mm circular disks and 100 mm × 35 mm × 0.6 mm slices at a temperature of 200°C.

Gel Permeation Chromatography (GPC)

The MW and molecular weight distribution of the raw materials used were tested by Model PL-GPC 220, UK. 1, 2, 4-trichlorobenzene was used as solvent and the test temperature was 160°C. All the data were calibrated using polystyrene standard.

Dynamic Rheology Analysis

Frequency (0.01–100Hz) scan of all the samples were performed using an AR ex2000 dynamic rheometer. The temperature was 170°C and the strain was 1%.

DSC Tests

The calorimetric experiments were performed in TA Q20 DSC calibrated with indium. All the following DSC scans were conducted in a nitrogen atmosphere. The cooling and heating rate of all standard DSC and SSA tests was 10°C/min. Samples of about 5 mg were used for the tests.

(1) Standard DSC test: initial temperature was set at 40°C. The samples were firstly heated to 160°C and held at 160°C for 5min to erase any thermal history. After that, the samples were cooled to 40°C and then heated to 160°C to get cooling and heating curves, respectively.
(2) SSA test: after melting the samples at 160°C for 5 min to erase previous thermal history, a "standard" thermal history was created by cooling them down to 40°C; then heating the samples to the first self-nucleation temperature 134°C and holding 5 min for isothermal crystallization. After that, the samples were cooled down to 40°C, and were heated once again to the second self-nucleation temperature 131°C and after 5 min isothermal procedure cooling the samples down to 40°C. We chose one T_s every 3 °C in 134 −125 °C and every 5 °C in 125–100 °C, so eight thermal fraction temperatures in all was performed. Finally, SSA fractionation curves were obtained by melting the samples to 160°C. The first self-nucleation temperature was chosen carefully. It should be at the best self- self-nucleation temperature, i.e., Domain II of H0 sample which had the highest melting temperature. We chose to vary the fraction window in order to improve the fractionation effect.

EWF Test

The 100 mm × 35 mm × 0.6 mm slices were cut into DENT specimens. A fresh single side razor blade was used to cut the

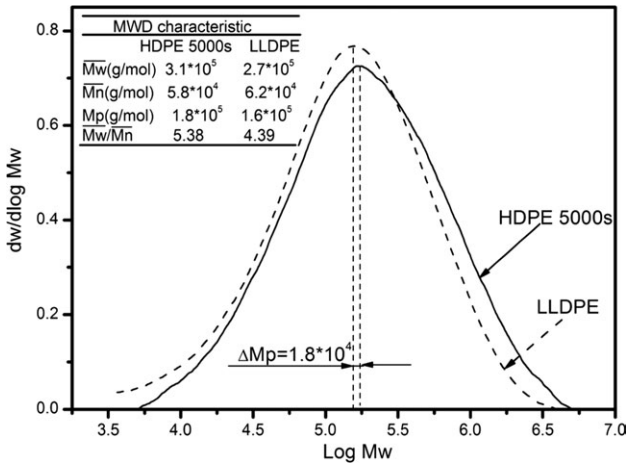

Figure 1. Molecular weight distribution curves of LLDPE and HDPE.

pre-cracks perpendicularly to the tensile direction. Ligament lengths were controlled to be between $W/3$ and $3t$ (W, t were the width and thickness of the specimens). Accurate ligament lengths and specimens thickness were measured using a microscope and a screw-thread micrometer. At least 20 specimens were made with distributional ligament length for each sample. Then all specimens were stretched using an Instron4302 universal test machine equipped with a 500 N load cell at a crosshead speed of 5 mm/min. Room temperature was 23±2°C. Total fracture energy could be obtained by integrating the recorded load-displacement curves.

RESULTS AND DISCUSSION

The Chain Structure Characteristics

Figure 1 shows the molecular weight distribution curves of the HDPE and LLDPE samples. There is almost no difference in the peak molecular weight (1.8×10^5 for HDPE and 1.62×10^5 for LLDPE) and the molecular weight distribution curve between the two raw materials. LLDPE sample has a slightly lower weight-average molecular weight and a slightly higher number-average molecular weight than HDPE, which means that the former has a narrower polydispersity index, but the difference is very small.

These small differences are hardly to be reflected on molecular weight distribution curves of the blends, or in other words, the blends still show normal Gaussian distribution in molecular weight, almost the same as the two raw materials. However, the major difference in these two raw materials is the chain branching content. LLDPE is an ethylene/1-butylene copolymer with a unimodal SCB distribution and the average SCB content is about $16CH_3/1000C$, while HDPE has a much lower Gaussian SCB distribution than LLDPE, mainly generated in the polymerization process. Therefore, it is reasonable to conjecture that the SCB distribution of the blends would show "bimodal" characteristic. Thus, compared to other normal BPE resin, this blend is of significance from the following aspects. (1) It is a PE materials with normally unimodal molecular weight distribution but a bimodal SCB distribution obtained by melt blending; (2) Its crystallization and mechanical behaviors due to this "bimodal chain branch distribution" characteristic are curious; (3)It can be used to examine the conclusions of previous works[5–12,18–20] which involve both molecule weight and chain branching differences, for example, by distinguishing/determining whether or not molecule segregation or segment segregation happens in the blend; (4) It may be a way to develop a new kind of PE blend with special structures and properties.

Dynamical Rheological Behavior

Dynamic rheology analysis was used to evaluate the homogeneity of all the samples at molten state. Based on molecular viscoelastic theory, Cole–Cole plot and Han curve (Figure 2) are sensitive for the phase separation of polymer systems.[37,38]

Normally, smooth and semicircular-shaped curve of η'' versus η', i.e., Cole–Cole curve indicates that the components are miscible, while un-smooth or bimodal curve show the phase separation in the blends.[39] As could be seen in Figure 2(a), all samples show nearly smooth and semicircular-shaped (except the very slight difference of H50 and H70), indicating good

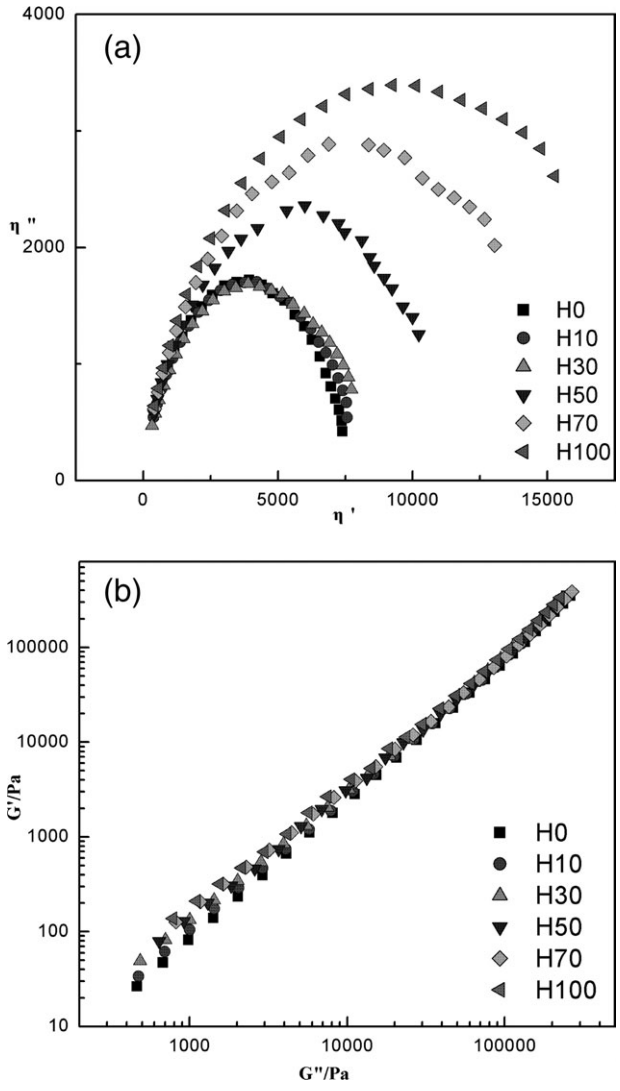

Figure 2. Dynamical rheological results of all HDPE/LLDPE samples: (a) Cole–Cole plots (b) Han plots.

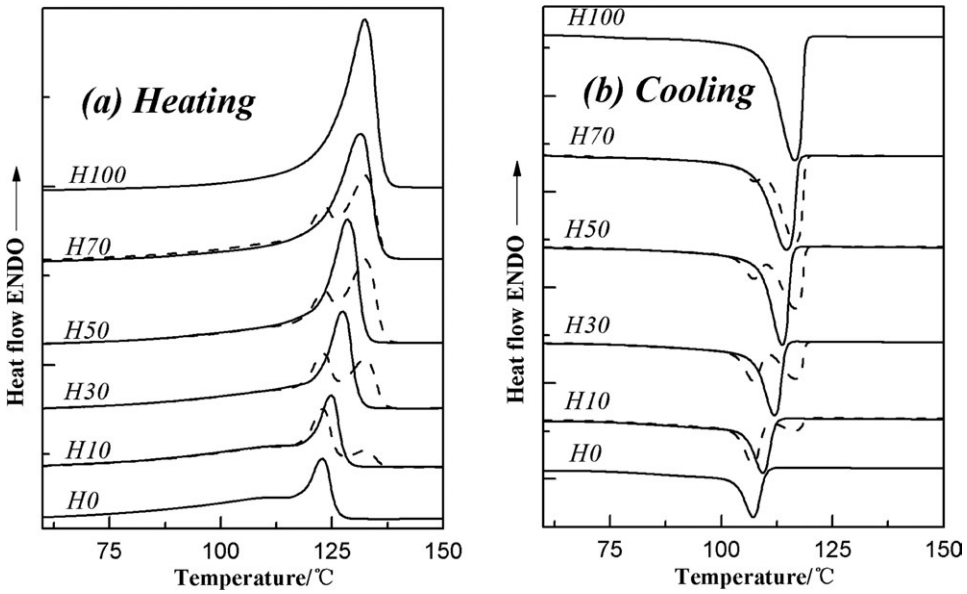

Figure 3. The (a) heating and (b) cooling curves of all HDPE/LLDPE samples in common DSC tests. Solid lines are actual curves and dashed lines theoretical 'unmixed' curves.

miscibility between the two components, even they are not absolutely miscible.

The relation of G' versus G″, namely Han plot, is also widely used to investigate the miscibility of polymer blends. For blends with good miscibility, Han plots are independent of the composition and good linearity and the same slope will be shown in all compositions. That is to say, the slope of Han plots is nearly constant for good miscibility polymer system only vary with different materials and do not change with varying test temperatures.[37,38] In Figure 2(b), all the Han plots at 170°C show neatly linearity with almost the same slope. In our system, we also performed this experiment at 150°C, and 190°C, no obvious different in the slope can be found. So, no evidence of immiscible or poor homogeneity is observed in the molten state for all the blends.

Crystallization Behaviors

Standard DSC Results. Figure 3(a) shows the DSC heating curves of HDPE/LLDPE blends in a common DSC heating procedure. The pure LLDPE (H0) sample shows a broad and low secondary melting endotherm at 110°C except the main endotherm at 117°C. LLDPE sample is poorer in molecular regularity and higher in branching content, so the melting endotherm at 110°C might correspond to imperfect lamellae formed by LLDPE chains with high SCB.[28] The pure HDPE (H100) sample has only one clear and sharp melting endotherm, with the peak melting temperature (T_m) being 10°C higher than that of LLDPE, apparently caused by the good chain regularity.

Significant differences can be seen between actual curves and the theoretical "unmixed" curves [dashed lines in Figure 3(a)]. The later can be seen as responses from DSC of two homopolymers which are completely immiscible. Apparently, the theoretical curves have two main endotherms, corresponding to those of LLDPE and HDPE components, respectively, while actual curves of the blends show only one main melting peak, located in the middle of the two melting endotherms of the theoretical ones.

Figure 3(b) shows that the variations of the cooling curves of the blends are similar with those of the heating curves. Only one exotherm can be seen in all the samples, while two clear exotherms are shown in the theoretical curves. Early researches regarded this as a signal of co-crystallization,[10,13] but it also might be caused by the overlapping of molten or crystallization peaks.

The dependences of T_m, peak crystallization temperatures (T_c), and crystallinity (X_c) on HDPE content is presented in Figure 4. Apparently that X_c has a good linear relationship with the blend

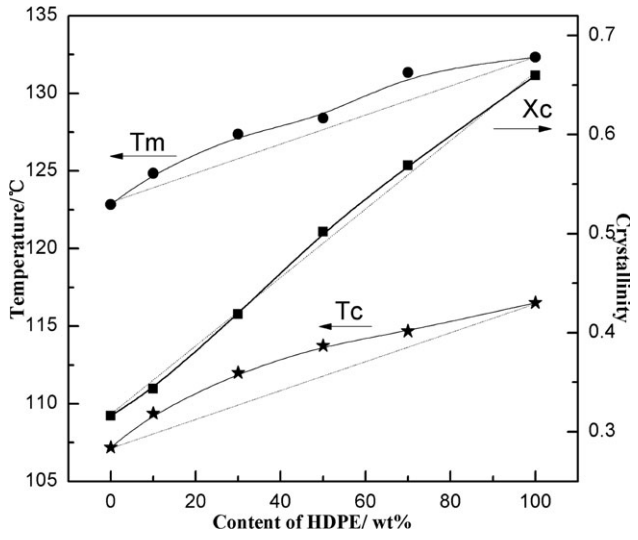

Figure 4. The dependency of melting point (T_m), crystalline temperature (T_c), and crystallinity (X_c) with the blend composition.

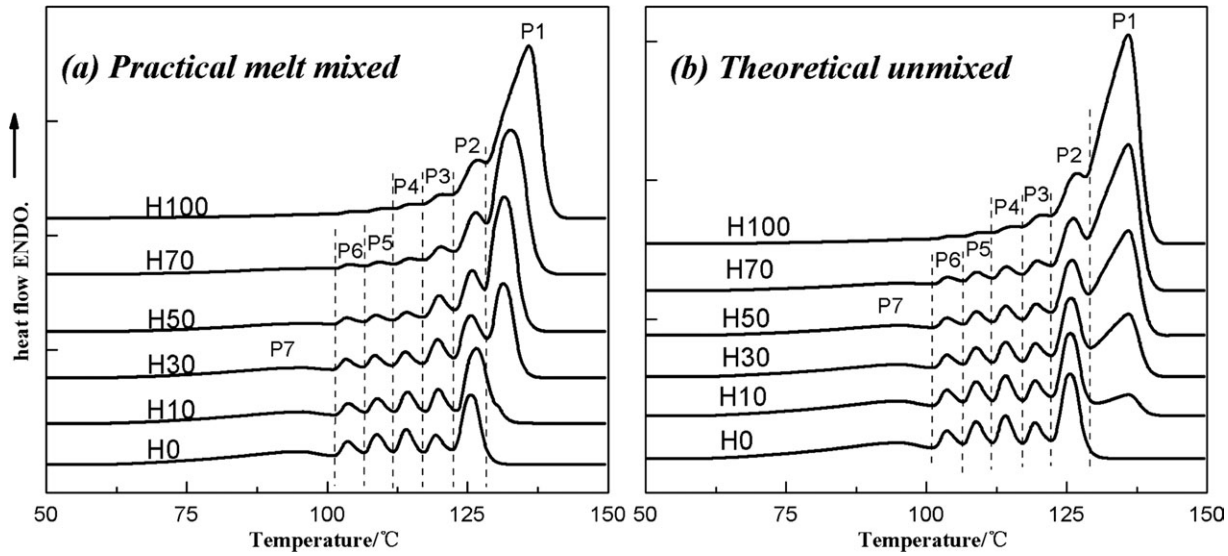

Figure 5. Final heating curves of all the samples after SSA thermal fractionation: (a) practical curves and (b) theoretical 'unmixed' curves.

composition, which is accordance with Krumme et al.[10] However, the variations of T_m and T_c show a positive deviation rather than linear increase with the increase of HDPE content. From H0 to H10, 10% increase of HDPE content causes a 3.1°C increase in T_m and a 2.3°C increase in T_c. When the content of HDPE is above or equal 50%, T_c and T_m have a little change. Similar phenomenon was also found by Arnal et al.[28] and could come to the conclusion that HDPE plays a decisive role on T_m and T_c of the blends.

There are two main possible interactions that might lead to the phenomena revealed in common DSC tests. (1) The combination influence of a "nucleation effect" of the HDPE component on the LLDPE component and a "dilution effect" of the LLDPE component on the HDPE component.[17,28] The "nucleation effect" increases the T_m and T_c of LLDPE crystals, while the "dilution effect" may cause the decrease in T_m and T_c of HDPE component. (2) On the other hand, there also exists a possibility that the HDPE chains could co-crystallize with the more linear fraction of the LLDPE component. During crystallization, all PE materials share the same crystalline unit, i.e., the methylene sequence. So it is very likely that the linear part of LLDPE which has similar methylene sequence length (MSL) can co-crystallize with HDPE chains since they are partially miscible and the influence of molecular weight is excluded in our system.

Further investigating method is needed to tell if the "nucleation and dilution effect" or/and co-crystallization is the prevailing interaction in our HDPE/LLDPE blends.

SSA Results. The SSA method has its unique advantage in detecting the crystallization behavior of PE samples than common DSC test.[28–31] After SSA treatment, each peak is supposed to be corresponding to the melting signal of lamellae formed by chains with similar MSL. Chains with longer MSL will form thicker lamellae and melt at a higher temperature. A completely linear PE sample with no detectable chain branch will show only one melting signal even after SSA treatment,[28,29] while pure LLDPE would show clearly a multi peaks curve. In our 'bimodal chain branch distribution" PE blend system, SCB distribution become the only varying molecular parameter affecting MSL and MSL distribution since the two raw materials have the almost the same molecular weight distribution curve. In this way, the variations in SSA curves are reflections of SCB situation undoubtedly.

Final heating curves of all the samples after SSA treatment are shown in Figure 5(a). Melting peaks with the similar position along the temperature axis are marked as P_i from the high temperature to the low temperature. The peak temperatures of each fraction and its corresponding annealing temperatures (T_s) are listed in Table I. In the case of pure HDPE, except for the

Table I. Peak Temperature P_i(°C) and Crosponding T_s (°C) of Each Melting Peak in SSA Final Heating Curves of all HDPE/LLDPE Samples

	T_s	H0	H10	H30	H50	H70	H100
P_1	125	-	-	131.4	131.7	132.8	135.9
P_2	120	125.5	126.7	125.6	125.8	126.2	126.2
P_3	115	119.2	119.7	119.7	119.9	120.2	120.0
P_4	110	114.1	114.2	113.8	114.1	114.4	-
P_5	105	108.9	108.9	108.5	108.7	109.1	-
P_6	100	103.5	103.6	103.2	103.5	103.8	-
P_7		94.7	95.4	95.6	95.7	-	-

Applied Polymer SCIENCE

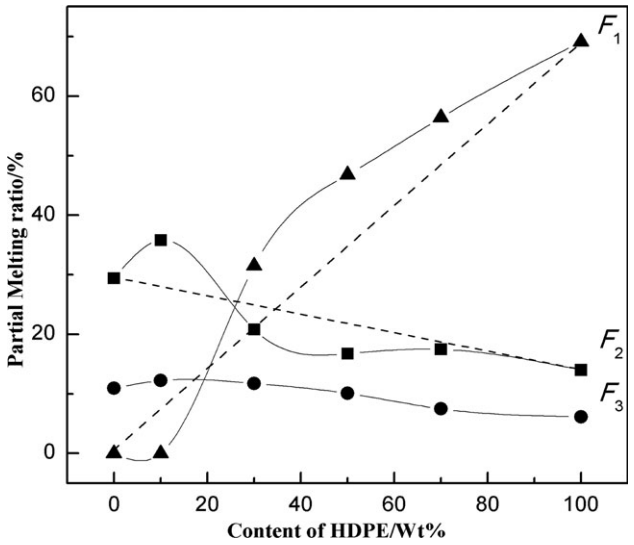

Figure 6. The partial area ratios (the ratio of P_i area to total area) of the first, the second, and the third lamella population (namely F_1, F_2, and F_3) variation with the blends composition.

highest and strongest melting peak i.e. P_1 at 135.9°C corresponding to the thickest lamella population annealed at T_s = 125°C, there are also three unshaped peaks (P_2, P_3, and P_4) at 126.2, 120.0, and 114.4°C, corresponding to lamellae annealed at 120, 115, and 110°C, respectively. This result indicates that the pure HDPE sample we used here is not a purely linear PE sample, but a sample with a small degree of SCB (about 3 CH_3/1000C). On the other hand, pure LLDPE have more clear melting peaks at lower temperature, and its highest melting peak [i.e. P_2 in Figure 5(a), corresponding to its first annealing T_s, 120°C] is much lower than that of HDPE. It should be noticed that P_7 (with a peak temperature of 95°C) of all the samples rich in LLDPE are not the melting signals of lamellae formed during the isothermal process at any T_s but caused by melting of crystals formed by LLDPE chains with the highest SCB content in the dynamic cooling process from the last T_s (100°C). Also, at fractionation temperatures higher than 125°C for H30–H100 and 120°C for H0–H10, only a self-nucleation process is carried out for all the samples with no fractions go though annealing. In all, the HDPE sample has four fraction peaks with a very low degree of SCB, and the LLDPE sample has five fraction peaks with a much higher degree of SCB and broader SCB distribution. Therefore, the two samples can indeed be mixed together to product a "bimodal chain branch distribution" PE sample.

Figure 5(b) shows the "theoretical unmixed" curves of all samples, which was achieved by simulation (via mathematical method). It could be seen as the expected behavior of HDPE/LLDPE blends in SSA test, with the absence of any interactions between the two components. Clearly differences can be found between the practical curves and the theoretical ones. In Figure 5(b), all the blends have melting signals at P_1 with almost the same peak temperature. However, in practical curves, a very clear melting point depression can be observed on the peak temperatures of P_1 from pure HDPE to 30% HDPE sample (as we will discuss later, there is no P_1 in the SSA curve of H10 sample), and it seems 30% of LLDPE would have a remarkable influence on the peak temperatures of P_1 (decrease by 3.1°C from H100 to H70), indicating that "dilution effect" becomes the significant interaction between the two components, and this "dilution effect" is more effective when the blend has higher HDPE content.[8,17,28]

Another dramatically difference is, the H10 sample does not have a melting endotherm at P_1. The SSA curve of H10 is very like that of pure LLDPE, except that the area of P_2 is larger. Arnal et al.[28] assumed that the missing of melting peaks in SSA test is a symbol of co-crystallization in High LLDPE content blends. In their study, even all samples showed clearly a "dilution effect", no missing of P_1 was shown in the SSA curves of blends of unbranched HDPE with LLDPE; while for the blends of branched HDPE with LLDPE, no P_1 could be observed in a large range of HDPE content (30% and lower). They then regarded that only the "dilution effect" operated in the former

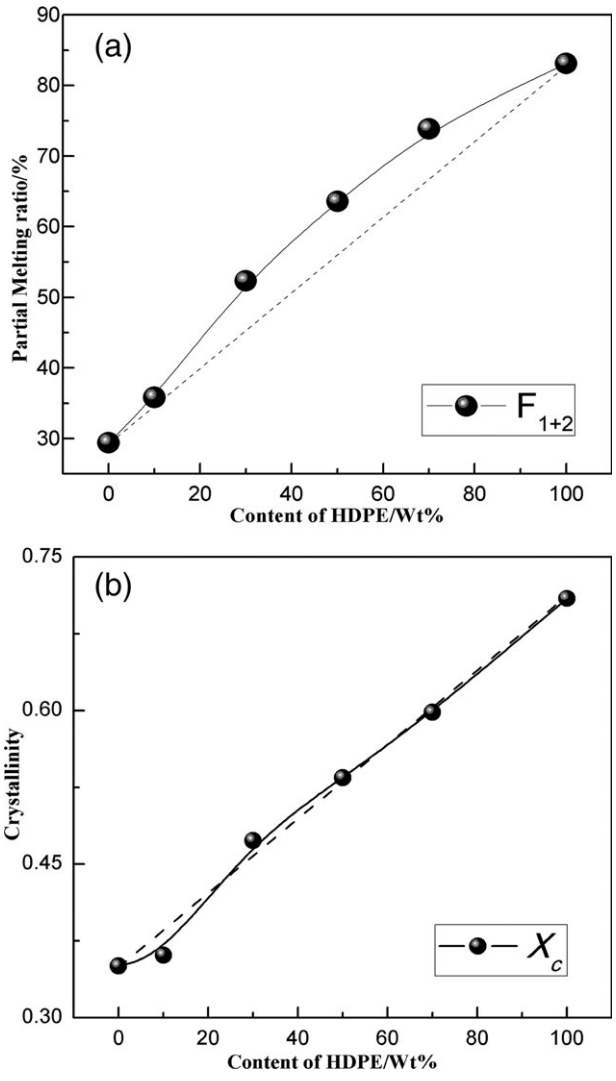

Figure 7. The dependence of (a) partial melting ratio of the highest two melting peaks (the ratio of P_1+P_2 area to total area) and (b) total crystallinity after SSA thermal fractionation on the composition of the blends.

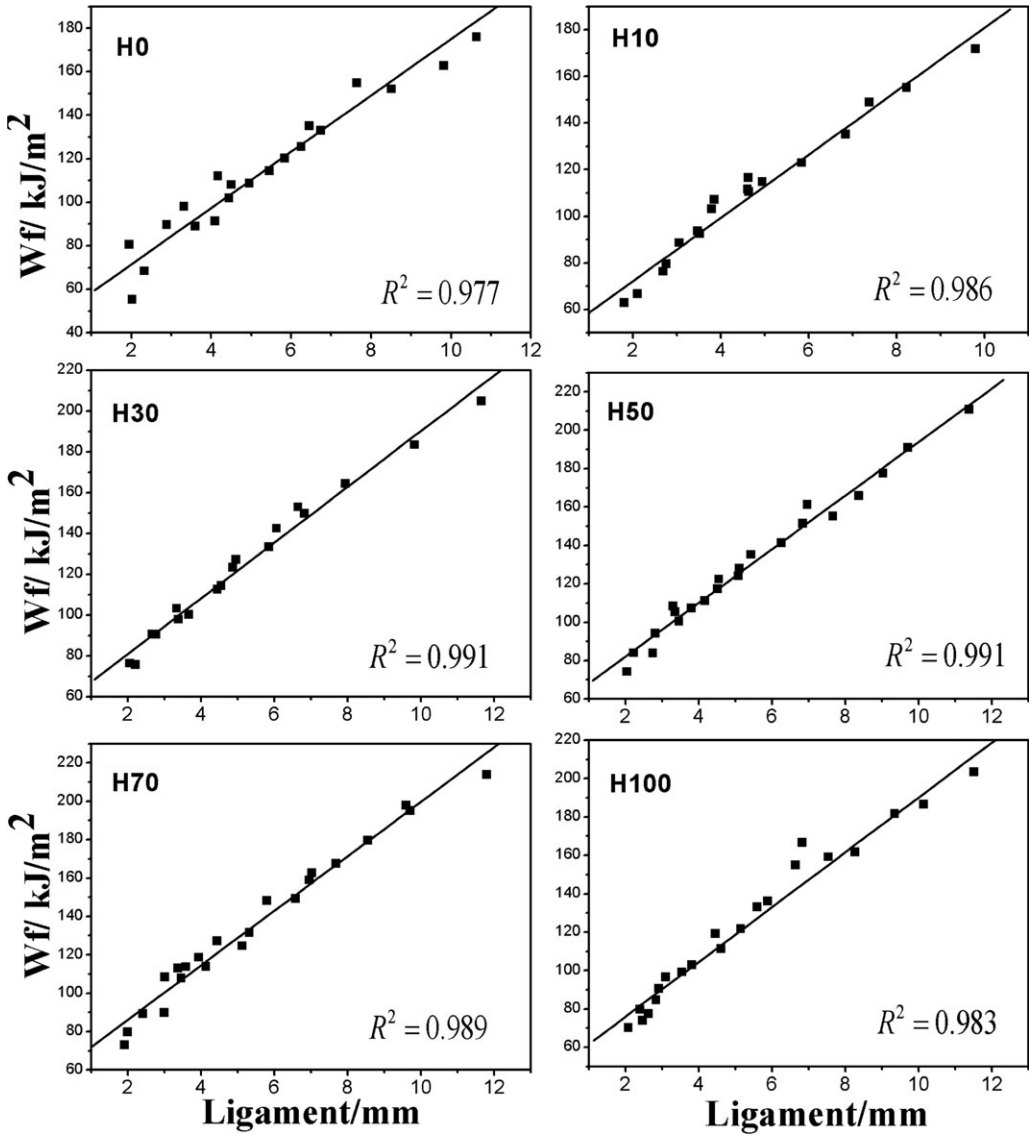

Figure 8. The w_f–l curves and linearly dependent coefficients (R^2) of all HDPE/LLDPE samples.

system; while in the latter, for blends with 30% and lower HDPE content, the fraction of HDPE which was supposed to be fractionated at P_1 co-crystallized with the most linear fraction of LLDPE and the co-crystals were so stable that could not be fractionated even after the SSA treatment.[28] In H10 sample of our system, the co-crystals contain more LLDPE segments and tend to show the characteristics of LLDPE component with slightly influence from HDPE component. This is why the melting signal at P_1 vanishes and the peak temperature of P_2 is higher than that of the other samples (see Table I).

The area under each peak is supposed to reflect the content of corresponding lamella population, and is also largely influenced by co-crystallization between the two components. The SSA curves were divided into separate fractionations by drawing base lines connecting the adjacent valleys to calculate the area of each fraction (abbr. F_i). Figure 6 shows the variations of partial area ratios of the first, the second, and the third lamella populations (namely F_1, F_2, and F_3) with the blends composition. Positive deviation of F_1 values and negative deviation of F_2 from the theoretical curves can be observed for H30, H50, and H70 sample. This is very likely owing to the reason that co-crystallization also exists for the blends with high HDPE content. This novel trend shown in Figure 6 was mainly due to the amount of chains participated in the co-crystallization and whether the co-crystals contribute its melting enthalpy to F_2 or F_1. The co-crystals contain two components, the more linear HDPE segments (the first lamella population) which should contribute its melting enthalpy to F_1 and the less linear LLDPE segments (the second lamella population) which should contribute its melting enthalpy to F_2. For H10 sample, the first lamella population co-crystallized with the second. The co-crystals contain much more LLDPE chains than linear HDPE chains, makes them not prefect enough to anneal at the first T_s and melt at P_1. Thus, the co-crystal contributed their melting enthalpy to F_2. This is why the H10 sample has its F_1 value equal to zero and F_2 much higher. In blends H30, H50, and H70, the

Applied Polymer SCIENCE

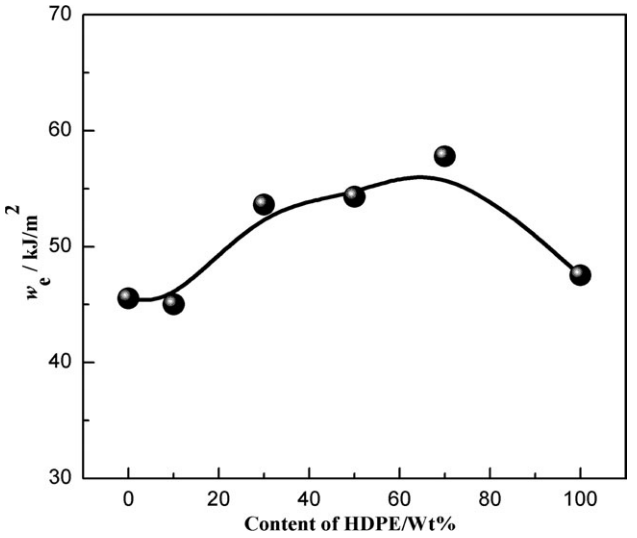

Figure 9. The variation of w_e with the blends composition.

co-crystal contains more linear segments since more HDPE chains participated in the co-crystallization and the co-crystals tend to contribute its melting enthalpy to F_1. Thus, the less linear parts participated in the co-crystallization (which should contribute its melting enthalpy to F_2) was induced to contribute its melting enthalpy to F_1 while the other part of the less linear parts didn't participated in the co-crystallization still contributed its melting enthalpy to F_2 as it should be. This is why F_1 become higher and F_2 lower than theoretical.

In all, for our "bimodal chain branch distribution" system, after overcoming the influence of molecular weight and molecular weight distribution, co-crystallization occurs in the blends of all the ratios and the co-crystals might show variational melting characteristics with different HDPE contents.

The thick lamellas, i.e., the first populations of lamella of pure HDPE and LLDPE (P_1 and P_2 respectively) after SSA treatments have contributed over 3/4 of the total crystallinity. A significant positive deviation can be seen in the variation of the partial area ratio of P_1+P_2 i.e. the thick lamella ratio (F_{1+2}) varies with HDPE content [Figure 7(a)], while the total degree of crystallinity linearly increases with blend composition [Figure 7(b)], which indicates no more uncrystalizable fragments take part in the crystallization . This means there exists a trend for crystalizable fragments to form more prefect lamellas. We should expect that the co-crystallization behavior and the trend for crystalizable fragments to form more prefect lamellas might have an obvious influence on the mechanical properties of the blends.

Fracture Behavior in EWF Tests

EWF method was used to evaluate the fracture behaviors of the blends. The total work of fracture (W_f), according to EWF theory,[40] can be written by related specific formulas:

$$W_f = W_e + W_p = w_e tl + \beta w_p tl^2 \quad (1)$$

$$w_f = W_f/tl = w_e + \beta w_p l \quad (2)$$

where W_e is the EWF applied to fracture the polymer in its process zone (surface-related), and W_p is plastic work consumed by various deformation mechanisms in the plastic zone (volume-related). The w_f, w_e, and w_p represent the specific total work of fracture, specific EWF and specific plastic work, respectively, and l is the ligament length, t the specimen thickness and β a factor related to the form of the plastic zone. βw_p is a constant, independent of l for certain material. By reading the ordinate intercept and the slope of the linear plot w_f vs l, w_e, and βw_p can be easily determined.

The load-displacement curves (not given here) of DENT specimens for all the samples show good self-similarity with typical yield and crack characteristics, and the good linear w_f–l relationships obtained are shown in Figure 8. All the appearances during the fracture process meet the pre-requisites of EWF tests.[40–42]

By extending the w_f–l curve to l =0, the value of w_e is obtained and shown in Figure 9. As can be seen in Figure 9, pure LLDPE (H0) has the least w_e (44.6 kJ/m^2), revealing that it has smaller ability to resist crack propagation than other samples. With the HDPE content increasing, w_e increases gradually until 57.8 kJ/m^2 for sample H70, 30% larger than that of sample H0. At the same time, the w_e of H70 is also 22% larger than that of pure HDPE sample (w_e = 47.4 kJ/m^2). No clear and regular change of the βw_p values can be observed for all the samples.

Normally, the fracture performance of semi-crystalline polymer is subjected to both the crystal perfection in crystalline region and the "tie molecule" amount in amorphous region, while the two are generally conflict to each other.[43]

For the crystal perfection in the crystalline region, as we expounded before in the SSA part, there exists a trend for crystalizable fragments to form more prefect lamellas. While in amorphous region, a certain degree of non-crystallizable LLDPE and HDPE contents ensures the amount of tie molecule. Such crystallization behaviors contribute to fracture performance of the blends evaluated by the EWF tests. With 10% HDPE incorporated, the co-crystallization occurs and the co-crystals tends to show the characteristics of LLDPE component with less increase in crystal perfection, thus, only a slight increase in w_e value were observed. While for H30, H50, and H70 samples with much higher w_e values than two raw materials, the exist of branching component and the fact that no more fragments take part in the crystallization than theoretical ensure the samples have sufficient number of tie molecules; the trend to form thicker lamella and the truth that co-crystals tend to show the characteristics of HDPE component guarantee that the blends have high extent of crystal perfection. In all, the co-crystallization behavior of our "bimodal chain branching distribution" PE blend system could promote the fracture toughness in effective ways.

CONCLUSIONS

"Bimodal chain branching distribution" HDPE/LLDPE blends with normal Gaussian molecular weight distribution were successfully obtained via melt blending. A certain degree of co-crystallization can be observed for all then blends even after

thermal fractionation and the crystal perfection was improved by the co-crystallization since there exists a trend for crystalizable fragments to form more prefect lamellas in the blends. In all, the co-crystallization behavior of our "bimodal chain branching distribution" PE blend system could promote the fracture toughness in effective ways. The w_e of H30, H50, and H70 are much higher than that of both pure LLDPE and HDPE. The sample H70 has the highest w_e, which is 30% and 22% higher than pure LLDPE and HDPE, respectively.

ACKNOWLEDGMENTS

The authors gratefully acknowledge the financial support from the National Natural Science Foundation of China (51073109).

REFERENCES

1. Elvers, B.; Hawkins, S.; Schulz. G. Ullman's Encyclopedia of Industrial Chemistry, 5th ed., VCH Publishers: New York, **1992**, 487.
2. Zhang, M.; Lynch, D. T.; Wanke, S. E. *Polymer* **2001**, *42*, 3067.
3. Junting, Xu.; Xurong, Xu.; Feng, L. *Eur. Polym. J.* **1999**, *36*, 685.
4. Wood-Adams, P. M.; Dealy, J. M. *Macromolecules* **2000**, *33*, 7489.
5. Shan, C. L. P.; Soares, J. B. P.; Penlidis, A. *Polymer* **2002**, *43*, 7345.
6. Shan, C. L. P.; Soares, J. B. P.; Penlidis, A. *Polymer* **2003**, *44*, 177.
7. Shen, H. W.; Luan, T.; Xie B. H.; Yang, W.; Yang, M. B. *J. Appl. Polym. Sci.* **2011**, *121*, 1543.
8. Sun, X.; Shen, H. W.; Xie, B. H.; Yang, W.; Yang, M. B. *Polymer* **2011**, *52*, 564.
9. Krumme, A.; Lehtinen, A.; Viikna, A. *Eur. Polym. J.* **2004**, *40*, 359.
10. Krumme, A.; Lehtinen, A.; Viikna, A. *Eur. Polym. J.* **2004**, *40*, 371.
11. Choi, P. *Polymer* **2000**, *41*, 8741.
12. Fan, Z. J.; Williams, M. C. Choi, P. *Polymer* **2002**, *43*, 1497.
13. Tashiro, K.; Stein, R. S.; Hsu, S. L.; *Macromolecules* **1992**, *25*, 1801.
14. Tashiro, K.; Satkowski, M. M.; Stein, R. S.; Li, Y. J.; Chu, B. Hsu, S. L. *Macromolecules* **1992**, *25*, 1809.
15. Tashiro, K.; Izuchi, M.; Kobayashi, M.; Stein, R. S. *Macromolecules* **1994**, *27*, 1221.
16. Cho, K.; LEE, B. H.; Hwang, K. M.; Lee, H.; Choe, S. *Polym. Eng. Sci.* **1998**, *38*, 1969.
17. Rana, S. K. *J. Appl. Polym. Sci.* **1998**, *69*, 2599.
18. Zhao, Y.; Liu, S. S.; Yang, D. C. *Macromol. Chem. Phys.* **1997**, *198*, 1427.
19. Tanem, B. S.; Stori, A. *Polymer* **2001**, *42*, 5389.
20. Tanem, B. S.; Stori, A. *Polymer* **2001**, *42*, 6609.
21. Starck, P.; Rajanen, K.; Löfgren, B. *Thermochim. Acta.* **2003**, *395*, 169.
22. Chen, F.; Shanks, R. A.; Amarasinghe, G. *Polymer* **2001**, *42*, 4579.
23. Anantawaraskul, S.; Soares, J. B. P.; Wood-Adams, P. M. *Macromol. Chem. Phys.* **2004**, *205*, 771.
24. Kong, J.; Fan, X. D.; Xie, Y. C.; Qiao. W. Q. *J. Appl. Polym. Sci.* **2004**, *94*, 1710.
25. Muller, A. J.; Hernandez, Z. H.; Arnal, M. L.; Sanchez, J. J. *Polym. Bull.* **1997**, *39*, 465.
26. Fazeli, N.; Arabi, H.; Bolandi, Sh. *Polym. Test.* **2006**, *25*, 28.
27. Anantawaraskul, S.; Soares, J. B. P.; Wood-Adams, P. M. *Adv. Polym. Sci.* **2005**, *182*, 1.
28. Arnal, M. L.; Sánchez, J. J.; Müller, A. J. *Polymer* **2001**, *42*, 6877.
29. Muller, A. J.; Arnal, M. L. *Prog. Polym. Sci.* **2005**, *30*, 559.
30. Arnal, M. L.; Balsamo, V.; Ronca, G.; Sánchez, A.; Müller, A. J.; Cañizales, E.; Urbina de Navarro, C. *J. Therm. Anal. Calorim.* **2000**, *59*, 451.
31. Lorenzo, A. T.; Arnal, M. L.; Muller, A. J.; de Fierro, A. B.; Abetz, V. *Macromol. Chem. Phys.* **2006**, *207*, 39.
32. Kwon, H. J.; Jar, R. Y. B. *Polym. Eng. Sci.* **2007**, *47*, 1327.
33. Lach, R.; Schneider, K.; Weidisch, R.; Janke, A.; Knoll, K. *Eur. Polym. J.* **2005**, *41*, 383.
34. Yang, W.; Xie, B. H.; Shi, W.; Li, Z. M.; Liu, Z. Y.; Chen, J.; Yang M. B. *J. Appl. Polym. Sci.* **2006**, *99*, 1781.
35. Choi, B. H.; Demirors, M.; Patel, R. M.; deGroot A. W.; Anderson K. W.; Juarez V. *Polymer* **2010**, *51*, 2732.
36. Lorenzo, A. T.; Arnal, M. L.; Muller, A. J., Lin, M. C.; Chen, H. L. *Macromol. Chem. Phys.* **2011**, *212*, 2009.
37. Utracki, L. A. Two Phase Polymer Systems; Hanser Publishers: Munich, **1991**.
38. Han, C. D.; Kim, J. K. *Polymer* **1993**, *34*, 2533.
39. Hameed, T.; Hussein, I. A. *Macromol. Mater. Eng.* **2004**, *289*, 198.
40. Bárány, T.; Czigány, T.; Karger-Kocsis, J. *Prog. Polym. Sci.* **2010**, *35*, 1257.
41. Williams, J. G.; Rink, M. *Eng. Fract. Mech.* **2007**, *74*(7), 1009.
42. Pegoretti, A.; Castellani, L.; Franchini, L.; Mariani, P.; Penati, A. *Eng. Fract. Mech.* **2009**, *76*, 2788.
43. Viana, J. C.; Cunha, E. M. *Adv. Mater. Forum Iii Pts 1 and 2.* **2006**, *514–516*, 1186.